Materials Science and Engineering C 51 (2015) 279–286

Contents lists available at ScienceDirect

Materials Science and Engineering C

journal homepage: www.elsevier.com/locate/msec

Synthesis and cytotoxicity of azo nano-materials as new biosensors for L-Arginine determination

Xuefang Shang [a,*], Leiming Luo [b], Kui Ren [a], Xiaofang Wei [c], Yaqian Feng [c], Xin Li [c], Xiufang Xu [d]

[a] Department of Chemistry, Xinxiang Medical University, Jinsui Road 601, Xinxiang, Henan 453003, China
[b] Department of Pharmacy, Third Affiliated Hospital of Xinxiang Medical University, Xinxiang, Henan 453003, China
[c] School of Pharmacy, Xinxiang Medical University, Jinsui Road 601, Xinxiang, Henan 453003, China
[d] Department of Chemistry, Nankai University, Tianjin 300071 China

ARTICLE INFO

Article history:
Received 28 January 2015
Received in revised form 3 March 2015
Accepted 8 March 2015
Available online 10 March 2015

Keywords:
Arginine
Biosensor
Nano-material
KYSE450

ABSTRACT

Inspired from biological counterparts, chemical modification of azo derivatives with function groups may provide a highly efficient method to detect amino acid. Herein, we have designed and prepared a series of azo nano-materials involving $-NO_2$, –COOH, $-SO_3H$ and naphthyl group, which showed high response for Arginine (Arg) among normal twenty kinds of (Alanine, Valine, Leucine, Isoleucine, Methionine, Aspartic acid, Glutamic acid, Arginine, Glycine, Serine, Threonine, Asparagine, Phenylalanine, Histidine, Tryptophan, Proline, Lysine, Glutamine, Tyrosine and Cysteine). Furthermore, theoretical investigation further illustrated the possible binding mode in the host-guest interaction and the roles of molecular frontier orbitals in molecular interplay. In addition, nano-material **3** exhibited high binding ability for Arg and low cytotoxicity to KYSE450 cells over a concentration range of 5–50 μmol · L^{-1} which may be used a biosensor for the Arg detection in vivo.

1. Introduction

With the increasing attention of host-guest chemistry, recognition and sensing of various molecular and ionic analytes have recently emerged as a key research field [1–22]. In particular, the detection of amino acid using biosensor has received an increased interest because amino acids, as the building blocks for proteins, play vital roles in the metabolic processes with living bodies [23–25]. As an important amino acid, Arginine (Arg) plays important roles in cell division, the healing of wounds, the removal of ammonia from the body, the function of the immune system, the releasing of hormones, and in particular, gene regulation, glycoprotein targeting, and vesicle transport [26]. Consequently, the selective recognition of Arg is crucial in the fields of biochemistry and medical science.

Detection methods for Arg have been reported based on traditional determination, such as HPLC, gas phase chromatography, ion exchange chromatography, electrochemical method, etc. [27,28]. The above methods have some deficiency, such as the expensive instruments, the poor repetitiveness and selectivity. The design and synthesis of artificial receptors arise more attention due to high selectivity for the analytes. In this regard, fluorescence is a vital detection method because of its simplicity and high sensitivity [29,30]. Even though considerable efforts have been devoted to develop fluorescent chemosensors for various guests, there have been relatively few reports on Arg selective receptors which show the fluorescent changes or color changes.

Azobenzol derivative is an important organic material and shows unique optical function [31]. As a potential host, azobenzene has been broadly exploited in many areas because of its efficient inclusion ability and easy derivatization by functional groups [32]. In addition, receptors containing aldehyde group show sensitive response for Arg according to literature [33]. Recently, reports of nano-materials are numerous due to their outstanding features in biological environment [34–36]. However, there are few reports about the application of small organic nano-material on the detection of amino acid.

In addition, Arg has an outstanding basicity attributed to its guanidine moiety, which can form a hydrogen-bonding interaction [37]. Based on the above consideration, we synthesized a series of azo derivatives containing aldehyde groups (Scheme 1) and prepared their nano-materials. The detection of amino acid using these biosensors was also studied in neutral aqueous solution and cell cytotoxicity of five nano-materials was evaluated on KYSE450. Results indicated that these nano-materials showed high response for Arg among normal amino acids tested (Alanine, Valine, Leucine, Isoleucine, Methionine, Aspartic acid, Glutamic acid, Arginine, Glycine, Serine, Threonine, Asparagine, Phenylalanine, Histidine, Tryptophan, Proline, Lysine, Glutamine, Tyrosine and Cysteine).

2. Material and methods

All reagents and solvents used were of analytical grade and most of the starting materials, especially for all amino acids, were purchased

* Corresponding author.
E-mail address: xuefangshang@126.com (X. Shang).

http://dx.doi.org/10.1016/j.msec.2015.03.005
0928-4931/

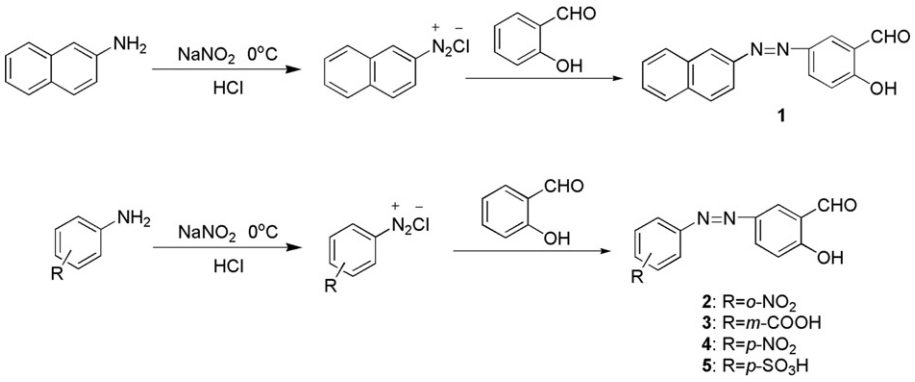

Scheme 1. Synthesis route for compounds.

from Aladdin Chemistry Co. Ltd (Shanghai, China). All amino acids were stored in a desiccator under vacuum, and used without any further purification. Dimethyl sulfoxide (DMSO) was distilled in vacuum after being dried with CaH_2. C, H, and N elemental analyses were made on a Vanio-EL instrument. ^{1}H NMR spectra were recorded on a Unity Plus-400-MHz spectrometer. ESI-MS was performed with a Mariner apparatus. UV–vis titration experiments were made on a Shimadzu UV2550 Spectrophotometer at 298 K. Fluorometric titration was performed on a Cary Eclipse Fluorescence Spectrophotometer at 298 K. The SEM images were obtained by Quanta TM450 FEI coating it with Au. The optimized geometries of compounds were used density functional theory at the B3LYP/3-21G level with Gaussian03 program. The binding constant, K_s, was obtained by non-linear least squares calculation method for data fitting.

Compounds **1**–**5** were synthesized according to the route shown in Scheme 1.

5 − (2′ − Azo − naphthalene) − salicylaldehyde (1)

5-(2′-Azo-naphthalene)-salicylaldehyde was synthesized according to the literature [38]. HCl (37%, 6 mL) was added slowly to a solution of 2-amine-naphthalene (5 mmol, 715 mg) in a small quantity of water at 0–5 °C. Then, $NaNO_2$ (20%, 20 mL) was added to the above-mentioned mixture and the solution was stirred for 1 h to give a bright yellow solution. Salicylaldehyde (5 mmol) dissolved in the solution of Na_2CO_3 (18 g Na_2CO_3 and 150 mL H_2O) was added dropwise to the bright yellow solution for 1 h. After stirring for 4 h, the reaction mixture was neutralized with HCl. The deep-red crude solid was filtered and recrystallized from ethanol to afford a pure product. Yield: 87%. ^{1}H NMR (400 MHz, DMSO-d_6, 298 K) δ 11.39 (s, 1H, –OH), 10.08 (s, 1H, –CHO), 8.92 (d, 1H, ph-H), 8.32 (dd, 2H, ph-H), 8.01–7.94 (dd, 2H, ph-H), 7.84 (d, 1H, ph-H), 7.69–7.56 (m, 3H, ph-H), 7.19 (d, 1H, ph-H). Elemental analysis: Calc. for $C_{17}H_{12}N_2O_2$: C, 73.90; H, 4.38; N, 10.14; Found: C, 73.88; H, 4.61; N, 9.84. ESI-MS (*m*/*z*): 275.3 (*M*-H)$^-$.

5 − (o − Nitro − phenylazo) − salicylaldehyde (2)

The synthesis method was similar to the above procedure. Yield: 77%. ^{1}H NMR (400 MHz, DMSO-d_6, 298 K) δ 11.47 (s, 1H, –OH), 10.02 (s, 1H, –CHO), 8.23–8.16 (m, 2H, ph-H), 7.94 (d, 1H, ph-H), 7.70 (d, 2H, ph-H), 7.61–7.58 (m, 1H, ph-H), 7.15 (d, 1H, ph-H). Elemental analysis: Calc. for $C_{13}H_9N_3O_4$: C, 57.57; H, 3.34; N, 15.49; Found: C, 57.73; H, 3.21; N, 15.67. ESI-MS (*m*/*z*): 270.2 (*M*-H)$^-$.

5 − (*m* − Carboxyl − phenylazo) − salicylaldehyde (3)

The synthesis method was similar to the above procedure. Yield: 91%. ^{1}H NMR (400 MHz, DMSO-d_6, 298 K) δ 13.32 (s, 1H, –OH), 11.64 (s, 1H, –CHO), 10.36 (s, 1H, ph-H), 8.33 (s, 1H, ph-H), 8.21 (s, 1H, ph-H), 8.14–8.07 (m, 3H, ph-H), 7.73–7.69 (t, sH, ph-H), 7.21 (d, 1H, ph-H). Elemental analysis: Calc. for $C_{14}H_{10}N_2O_4$: C, 62.22; H, 3.73; N, 10.37; Found: C, 61.94; H, 4.05; N, 10.56. ESI-MS (*m*/*z*): 269.4 (*M*-H)$^-$.

5 − (*p* − Nitro − phenylazo) − salicylaldehyde (4)

The synthesis method was similar to the above procedure. Yield: 73%. δ 11.48 (s, 1H, –OH), 10.06 (s, 1H, –CHO), 8.41 (d, 2H, ph-H), 8.30–8.21 (m, 2H, ph-H), 8.04 (d, 2H, ph-H), 7.18 (d, 1H, ph-H). Elemental analysis: Calc. for $C_{13}H_9N_3O_4$: C, 57.57; H, 3.34; N, 15.49; Found: C, 57.81; H, 3.59; N, 15.14. ESI-MS (*m*/*z*): 270.1 (*M*-H)$^-$.

5 − (*p* − Sulfonic − phenylazo) − salicylaldehyde (5)

The synthesis method was similar to the above procedure. Yield: 81%. ^{1}H NMR (400 MHz, DMSO-d_6, 298 K) δ 11.55 (s, 1H, –OH), 10.35 (s, 1H, –CHO), 8.18 (d, 1H, ph-H), 8.11–8.08 (dd, 1H, ph-H), 7.82–7.74 (m, 4H, ph-H), 7.20 (d, 1H, ph-H). Elemental analysis: Calc. for $C_{13}H_{10}N_2O_5S$: C, 50.98; H, 3.29; N, 9.15; Found: C, 50.61; H, 3.58; N, 8.99. ESI-MS (*m*/*z*): 304.2 (*M*-H)$^-$.

Nano-materials of five compounds were prepared by reprecipitation method [39,40]. The DMSO and the water solution of CTAB (hexadecyl trimethyl ammonium bromide) were good solvent and poor solvent, respectively. In the experiment, the good solvent containing compound (0.35 mL, 4 mmol·L^{-1}) was poured into the poor solvent containing CTAB (100 mL, 3 mmol·L^{-1}). The mixture was placed for 24 h and centrifuged. The expected solid was washed with water and dried in vacuum.

3. Results and discussion

3.1. SEM images of compounds

The SEM images were obtained by Quanta TM450 FEI coating it with Au (Fig. 1).

As shown in Fig. 1, compound **1** could be assembled into long-thin flakiness on the entire compound. The width of flakiness was nanometer according to the scale. Compound **2** was formed into an oval platelet. Two compounds (**3** and **4**) were both formed into ribbon although the substituent located in different positions. For compound **5** containing *o*-NO_2, it was assembled into flaky and like a flower entirely. Although compounds **2** and **5** have the same substituent (–NO_2), SEM images were remarkably different due to the different locations of nitro group. Therefore, SEM image was related with space configuration.

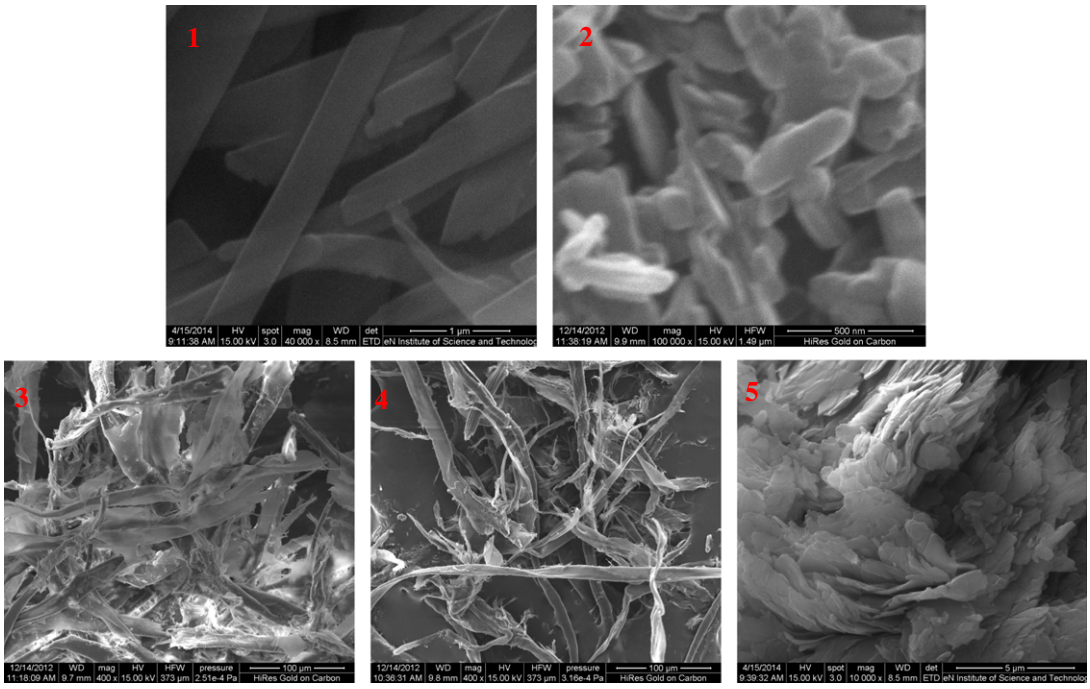

Fig. 1. SEM images for compounds.

3.2. UV–vis titration

The binding ability of five nano-materials with amino acid was investigated using UV–vis absorption spectra in DMSO-H_2O (1:1, v/v) at 298 K. The UV–vis spectral changes of five compounds were shown in Fig. 2 during the titration with Arg. In the absence of Arg, nano-material **1** (4.0×10^{-5} mol·L^{-1} in DMSO) exhibited an obvious peak at 398 nm. With the increase of Arg, the intensity of absorption peak at 398 nm strengthened remarkably and shifted to the long wavelength direction gradually. As a result, red-shift phenomenon occurred after compound **1** interacted with Arg. One clear isosbestic point appeared at 375 nm indicating the formation of stable complexation (**1**-Arg). Analogous investigations were carried out on other normal amino acids. The additions of Histidine, Asparagine, Lysine, Threonine and Tryptophan to compound **1** induced similar spectral change which indicated that compound **1** also interacted with the above amino acids. However, the additions of Proline, Leucine, Phenylalanine, Alanine, Glycine, Valine, Methionine, Aspartic acid, Glutamic acid, Isoleucine, Serine, Cysteine, Tyrosine and Glutamine did not induce any spectral response. The above results indicated that compound **1** showed no binding ability toward these amino acids (Fig. 3).

The acidity of this kind of compounds can be tuned by changing the electron property of the substituent on the ortho-, meta- or para-position according to resonance structure and the binding ability of amino acid can also be changed correspondingly [41]. Therefore, **2** (*o*-NO_2), **3** (*m*-COOH), **4** (*p*-NO_2) and **5** (*p*-SO_3H) were synthesized in order to investigate the effect of electron properties of substituent on the host–guest interaction. As expected, the absorption spectra of **2**, **3**, **4** and **5** indeed exhibited various changes with the increase of Arg concentration (Fig. 2). Furthermore, red-shift phenomena occurred in different degree and one clear isosbestic point also appeared which indicating five compounds all interacted with Arg. Compared with compounds **2**–**5**, the red-shift effect of compound **1** with Arg was not obvious which may be related with geometry. And the following theoretical investigation also proved the geometry of compound **1** was different with compounds **2**–**5**.

3.3. Fluorescent response

The photo physical responses of five nano-materials toward the additions of amino acids tested were also investigated in DMSO-H_2O (1:1, v/v) solution. As shown in Fig. 4, the fluorescence intensity of five compounds all increased with the stepwise addition of Arg. Two possible mechanisms may explain the fluorescent enhancement: (1) inhibition of photo-induced electronic transfer (PET) [42] and (2) the guest binding-induced rigidity of the host molecule [43,44]. For free nano-material, the oxygen atom of –CHO could form an intramolecular hydrogen bond with the hydrogen atom of the hydroxyl group (it could be proved by theoretical investigation), which led to a PET and a decreasement of fluorescence. However, the interaction between nano-material and Arg resulted in the inhibition of PET and an enhancing in the intensity of the fluorescent spectrum after the addition of Arg to the solution of nano-material. Similar fluorescence spectral changes of five nano-materials were induced by the additions of other studied amino acids. Nevertheless, their fluorescence emission was insensitive to the additions of large quantity of other amino acids which indicated that the interactions of host–guest were very weak and could be ignored.

3.4. Binding constant

Five nano-materials interacted with amino acids as the ratio of 1:1 or 1:2 according to the job-plot analysis. By the method of non-linear least squares calculation, the binding constants could be obtained and listed in Table 1 based on the UV–vis data [45–47]. From Table 1, five nano-materials all showed the strongest binding ability for Arg among amino acids tested. The reason may be that the aldehyde group of five nano-materials could interact with the guanidine group of the Arg through hydrogen bonding because of its outstanding basicity [26]. For other amino acids (Histidine, Asparagine, Lysine, Proline, Threonine, Leucine, Phenylalanine, Alanine, Glycine, Valine, Methionine, Tryptophan, Aspartic acid, Glutamic acid, Isoleucine, Serine), five compounds showed different binding abilities. However, five nano-materials

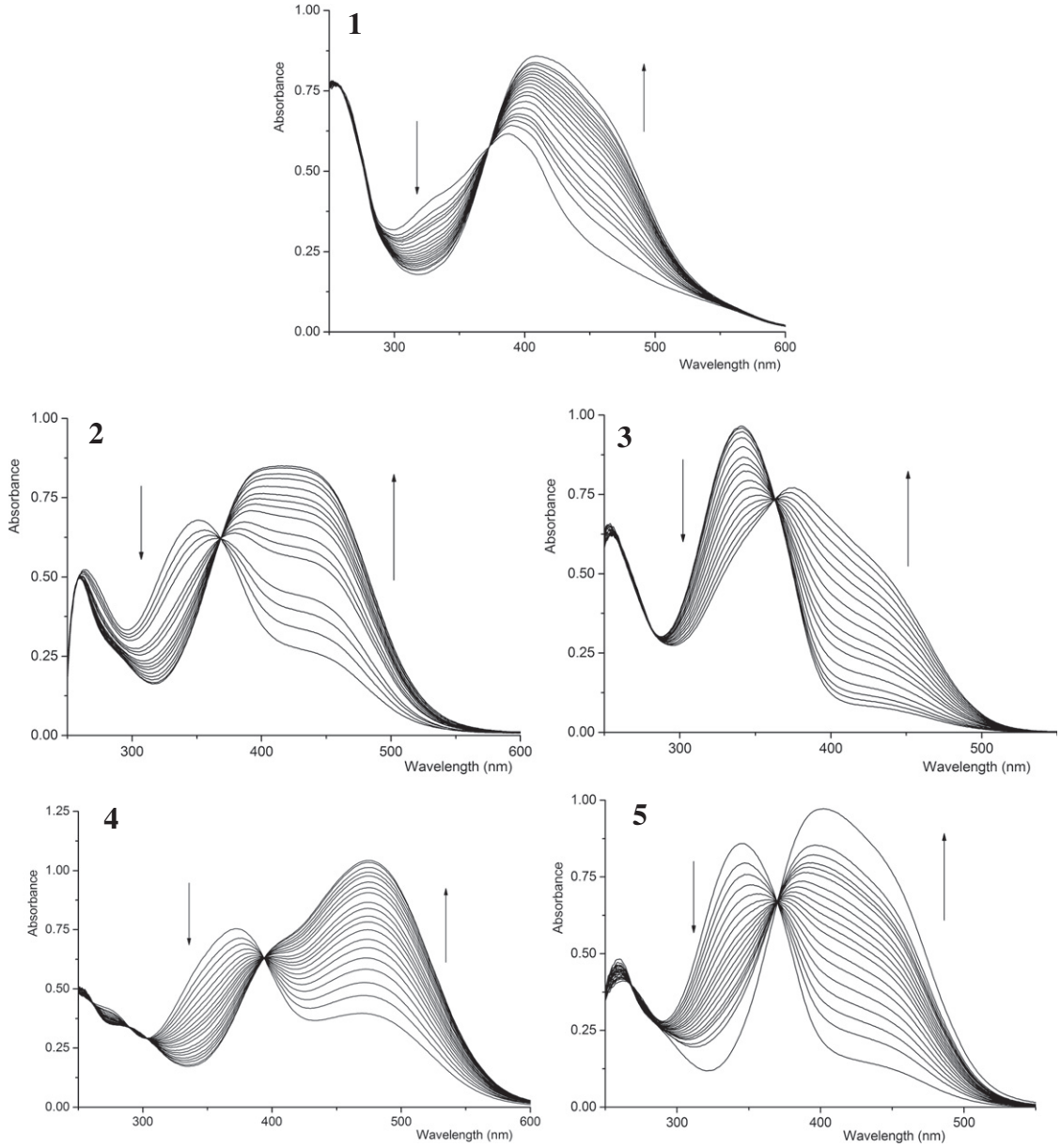

Fig. 2. UV–vis spectral changes of five compounds upon the addition of Arg. [compound] = 4.0×10^{-5} mol·L^{-1}; [Arg] = 0–1.6×10^{-3} mol·L^{-1}. Arrows indicate the direction of increasing anion concentration.

showed very weak binding ability for Cysteine, Glutamine and Tyrosine and could be ignored. The reason may be that π–π staking possibly existed between five nano-materials and amino acids. For Arg, the binding ability followed the order of: **3** > **2** > **1** > **4** > **5**. Compound **3** showed the strongest binding ability for Arg among five nano-materials. The reason may be the well match of space geometry and 1:2 binding ratio. In addition, the selectivity of compound **3** for Arg was the strongest among all compounds. Therefore, compound **3** could be used as a biosensor for the detection of Arg.

3.5. Theoretical investigation

To further understand the effect of aldehyde group on the photophysical properties, the geometries of five nano-materials and host–guest complexes (**3**-Arg) were optimized (Fig. 5) using density functional theory at the B3LYP/3-21G level with Gaussian03 program [48]. As shown in Fig. 5, the intramolecular hydrogen bond existed between the oxygen atom of –CHO and the hydrogen atom of hydroxyl group

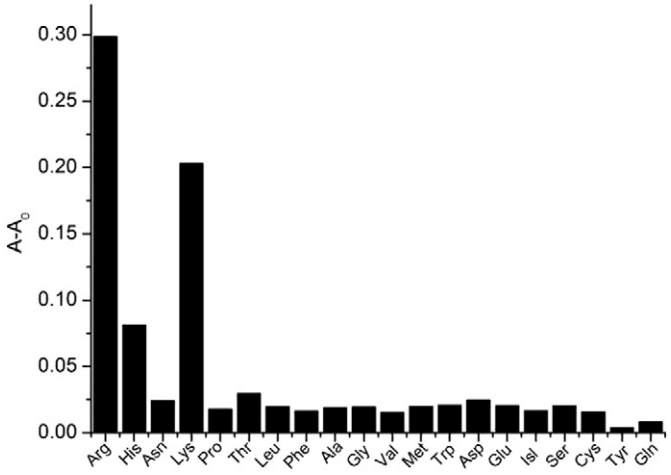

Fig. 3. UV–vis spectral changes of compound **1** upon the additions of various amino acids.

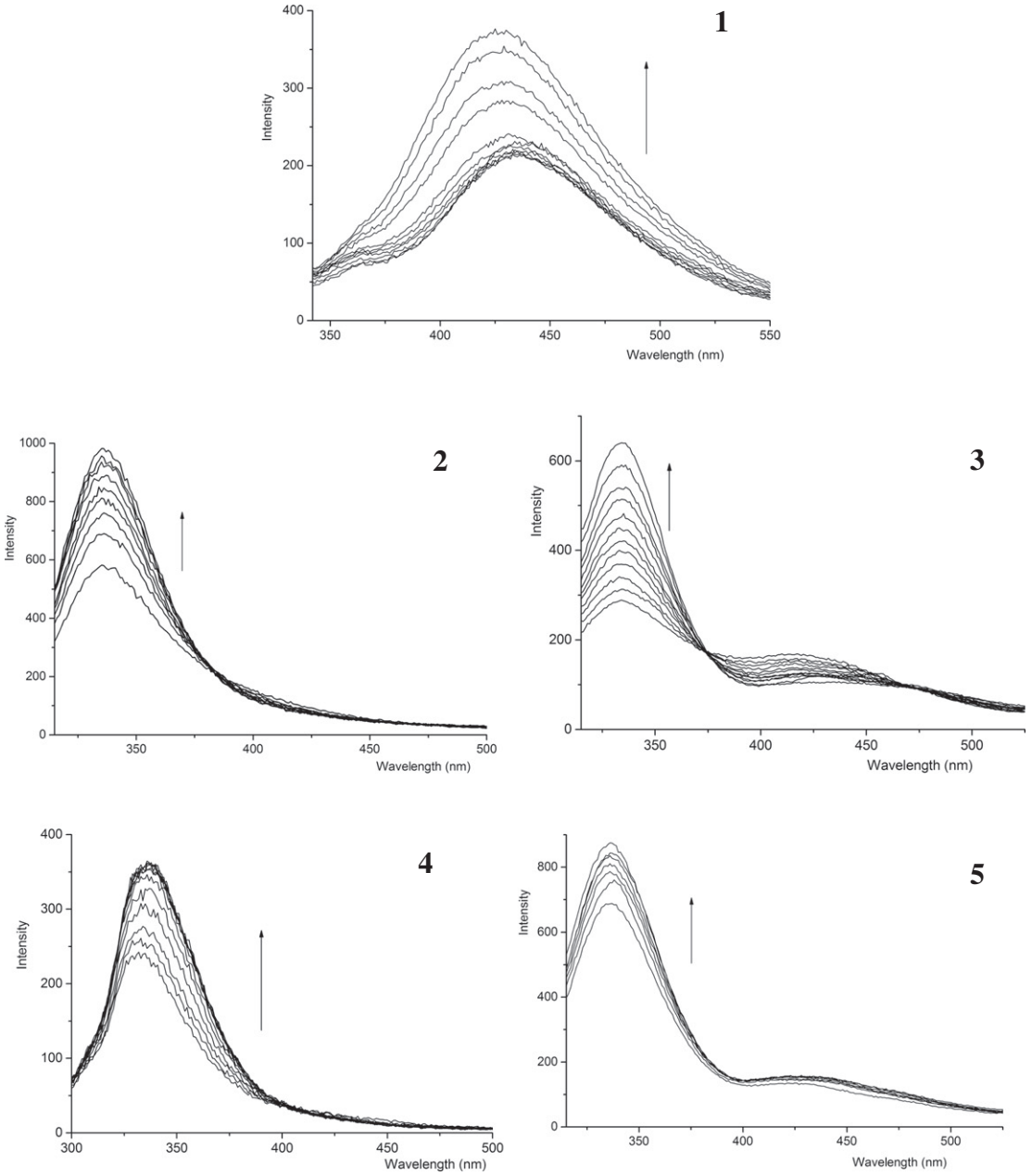

Fig. 4. Fluorescence response of five nano-materials (4.0×10^{-5} mol·L^{-1}) upon the addition of Arg (0–2.0×10^{-3} mol·L^{-1}), arrows indicate the increase direction of Arg concentration.

for compound **1**. However, the intramolecular hydrogen bond existed between the oxygen atom of –CHO and the near hydrogen atom of benzene for compounds **2**–**5**. The difference of intramolecular hydrogen bond induced the different red-shift effect in UV–vis spectra of host-guest. In addition, the geometry of the complexation between compound **3** and Arg was also optimized. Results indicated the intermolecular hydrogen bond existed between the oxygen atom of aldehyde group in compound **3** and hydrogen atom of amine group in Arg which proved aldehyde group was the binding site.

In addition, selected frontier orbitals for five compounds (**1**–**5**) were shown in Fig. 6. We introduced molecular frontier orbital in order to explain UV–vis absorption spectra in host–guest interacted process by electron transition of frontier orbital. Orbital analysis revealed that the highest occupied molecular orbital (HOMO) density in compounds **2**–**5** was mainly localized on the azo moiety, while the lowest unoccupied molecular orbital (LUMO) density was localized on the whole molecule. The above results indicated it was the electron transition of the highest HOMO to arouse the red-shift phenomenon in UV–vis spectra of **2**-Arg (or **3**-Arg, **4**-Arg, **5**-Arg). In contrast, the HOMO and LUMO distributions were located on the whole molecule for compound **1**. While, the LUMO density was correspond weak which indicated it was the LUMO to arouse the red-shift phenomenon in UV–vis spectra of **1**-Arg.

3.6. Cell cytotoxicity

Five nano-materials were evaluated for their anticancer activity in human cancer cell lines of esophageal carcinoma cell (KYSE450) by the MTT method (Fig. 7). It was found that nano-material **5** in the range 5–100 μmol · L^{-1} showed very low cytotoxicity, nano-materials **2** and **3** showed low cytotoxicity in the range concentration (<50 μmol · L^{-1}). However, nano-materials **1** and **4** were cytotoxic at the concentration (>30 μmol · L^{-1}). The cell viability of cells exposed to nano-materials **3** and **5** was minimally affected (90% cell viability). Combination with

Table 1
Binding constants of compounds with various amino acids.

Amino acid	K_s (**1**)	K_s (**2**)	K_s (**3**)	K_s (**4**)	K_s (**5**)
Arginine	$(1.28 \pm 0.04) \times 10^5$	$(1.09 \pm 0.03) \times 10^6$	$(2.76 \pm 0.02) \times 10^7$[b]	$(9.04 \pm 0.03) \times 10^4$	$(4.34 \pm 0.06) \times 10^4$
Histidine	$(8.20 \pm 0.15) \times 10^3$	$(2.39 \pm 0.02) \times 10^4$	$(2.12 \pm 0.03) \times 10^3$	$(9.94 \pm 0.68) \times 10^3$	$(3.85 \pm 0.08) \times 10^4$
Asparagine	$(3.31 \pm 0.07) \times 10^2$	$(6.12 \pm 0.04) \times 10^3$	$(6.13 \pm 0.06) \times 10^5$[b]	$(1.21 \pm 0.10) \times 10^4$	$(2.78 \pm 0.07) \times 10^3$
Lysine	$(8.30 \pm 0.04) \times 10^4$	$(1.03 \pm 0.02) \times 10^5$	$(1.04 \pm 0.34) \times 10^6$[b]	$(2.55 \pm 0.61) \times 10^4$	$(2.81 \pm 0.33) \times 10^4$
Proline	ND[a]	$(6.64 \pm 0.96) \times 10^2$	$(6.09 \pm 0.73) \times 10^4$[b]	$(9.57 \pm 0.69) \times 10^3$	$(2.09 \pm 0.03) \times 10^3$
Threonine	$(3.66 \pm 0.46) \times 10^2$	$(3.90 \pm 0.04) \times 10^3$	19.5 ± 7.9	$(8.15 \pm 0.57) \times 10^2$	$(1.02 \pm 0.09) \times 10^3$
Leucine	ND	$(3.45 \pm 0.02) \times 10^3$	ND	$(1.08 \pm 0.64) \times 10^3$	$(2.95 \pm 0.37) \times 10^3$
Phenylalanine	ND	$(4.71 \pm 0.73) \times 10^3$	ND	$(2.13 \pm 0.03) \times 10^3$	$(7.32 \pm 0.06) \times 10^3$
Alanine	ND	$(5.98 \pm 0.95) \times 10^3$	ND	$(2.00 \pm 0.03) \times 10^4$	$(2.01 \pm 0.63) \times 10^3$
Glycine	ND	$(5.79 \pm 0.83) \times 10^3$	ND	$(7.40 \pm 0.52) \times 10^3$	$(1.92 \pm 0.09) \times 10^3$
Valine	ND	$(6.64 \pm 0.80) \times 10^3$	ND	$(5.76 \pm 0.93) \times 10^3$	$(4.67 \pm 0.51) \times 10^2$
Methionine	ND	ND	ND	$(6.34 \pm 0.07) \times 10^3$	$(9.07 \pm 0.55) \times 10^3$
Tryptophan	$(3.50 \pm 0.03) \times 10^2$	ND	ND	$(1.60 \pm 0.06) \times 10^3$	$(4.59 \pm 0.07) \times 10^3$
Aspartic acid	ND	$(1.63 \pm 0.06) \times 10^5$	ND	$(1.32 \pm 0.04) \times 10^3$	ND
Glutamic acid	ND	$(7.83 \pm 0.42) \times 10^4$	ND	$(1.80 \pm 0.08) \times 10^3$	$(1.06 \pm 0.08) \times 10^3$
Isoleucine	ND	$(4.56 \pm 0.33) \times 10^3$	ND	$(3.58 \pm 0.30) \times 10^4$	$(2.09 \pm 0.07) \times 10^3$
Serine	ND	ND	ND	$(4.09 \pm 0.53) \times 10^4$	$(7.00 \pm 0.07) \times 10^2$
Cysteine	ND	ND	ND	ND	ND
Tyrosine	ND	ND	ND	ND	ND
Glutamine	ND	ND	ND	ND	ND

[a] The binding constant could not be determined.
[b] The binding ratio of host–guest is 1:2.

binding constants, nano-material **3** showed high binding ability and low cell cytotoxicity and may be used to detect Arg in vivo. Conversely, nano-materials **1** and **4** caused a remarkable decrease in cell viability at concentrations above 50 μmol · L^{-1}. The difference in cytotoxicity among five nano-materials was due to particle size, as well as the surface charge-to-volume ratio which were key parameters influencing interactions with cell membranes (through electrostatic attraction and hydrogen bonding) [49].

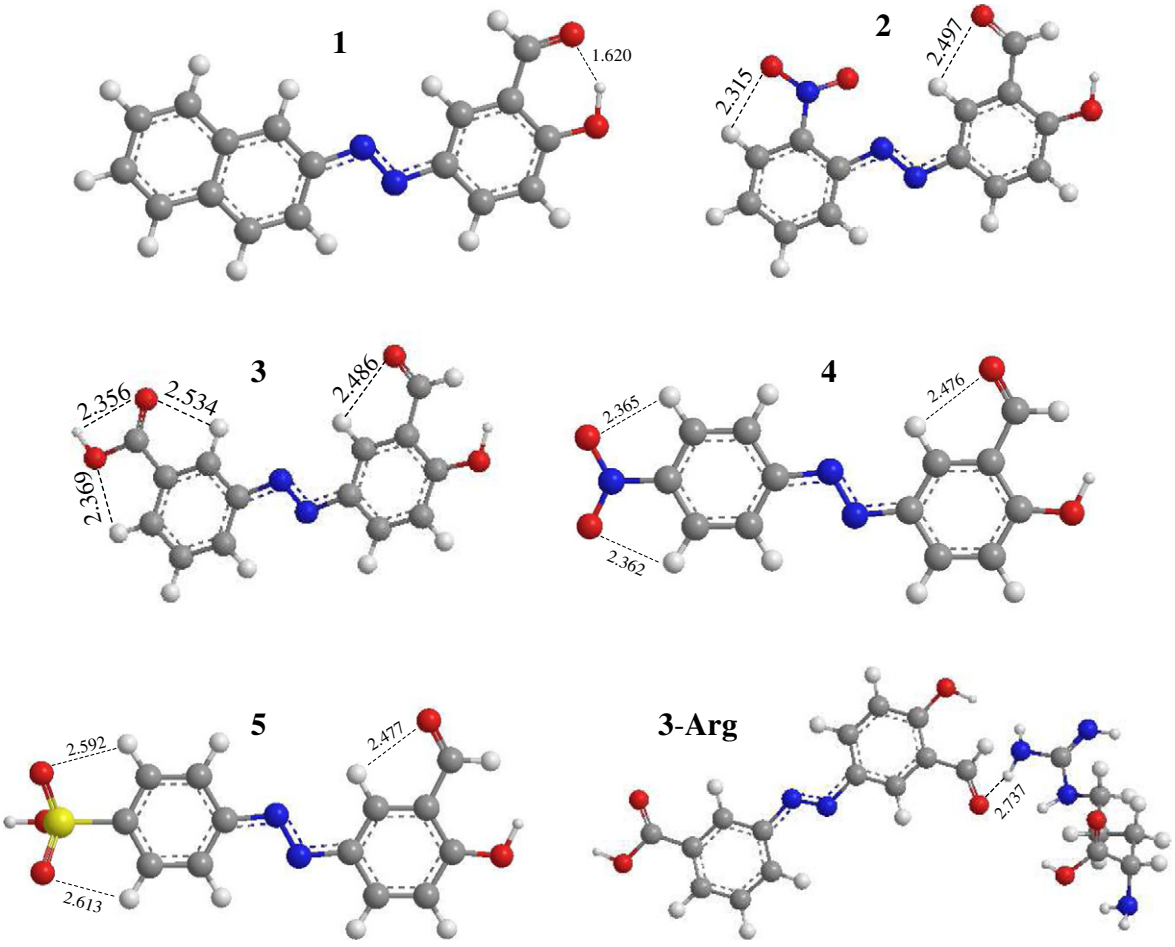

Fig. 5. Optimized structures of five compounds and **3**-Arg.

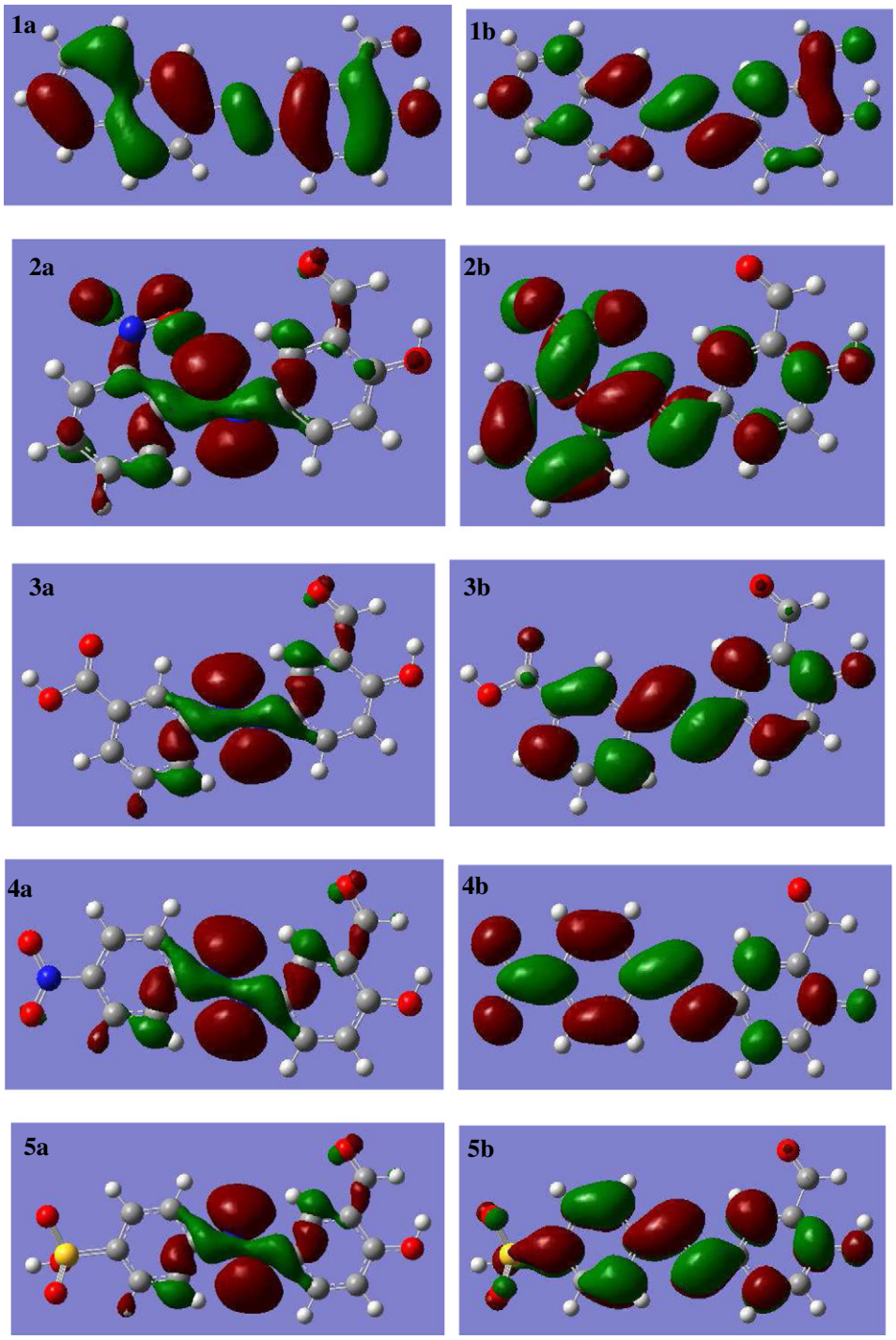

Fig. 6. Selected HOMO (a) and LUMO (b) distributions of **1**–**5.**

4. Conclusion

In conclusion, five nano-materials based on azo derivatives were developed and demonstrated a highly sensitive and selective absorption assay for Arg among twenty standard amino acids. Compound **3** containing *m*-COOH exhibited the strongest binding ability for Arg among five compounds and showed low cytotoxicity to KYSE450 cells over a concentration range of 5–50 μmol · L^{-1} which may be used as a biosensor for the Arg detection in vivo. This work is of great importance in gaining a better understanding of the special properties of azo derivatives in the presence of amino acids, and also greatly expands the scope of reagents which may find future application in the development of analytical methods for the selective determination of those amino acids such as Arg.

Acknowledgment

This work was supported by the National Natural Science Foundation of China (81301269) and Program for Science & Technology Innovation Talents in Universities of Henan Province (15HASTIT039).

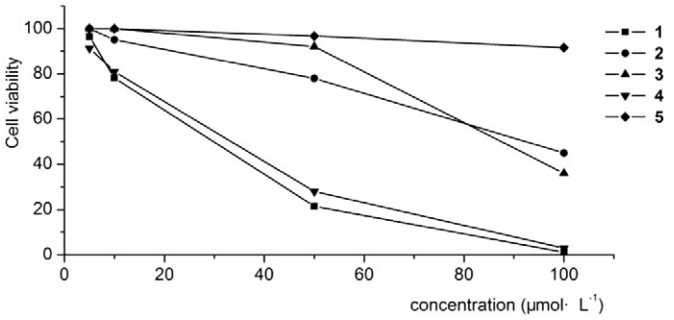

Fig. 7. Cytotoxicity profiles of five nano-materials on KYSE450 following 48 h incubation as determined by MTT assay. Data are presented as the average ± standard deviation (n = 5).

References

[1] L.E. Santos-Figueroa, M.E. Moragues, E. Climent, A. Agostini, R. Martínez-Máñez, F. Sancenón, Chromogenic and fluorogenic chemosensors and reagents for anions. A comprehensive review of the years, Chem. Soc. Rev. 42 (2013) (2010–2011) 3489–3613.

[2] S. Kado, H. Otani, Y. Nakahara, K. Kimura, Highly selective recognition of acetate and bicarbonate by thiourea-functionalised inverse opal hydrogel in aqueous solution, Chem. Commun. 49 (2013) 886–888.

[3] X.F. Shang, J.G. Du, W.C. Yang, Y. Liu, Z.Y. Fu, X.F. Wei, R.F. Yan, N.C. Yao, Y.P. Guo, J.L. Zhang, X.F. Xu, The development and amino acid binding ability of nano-materials based on azo derivatives: theory and experiment, Mater. Sci. Eng. C 38 (2014) 101–106.

[4] V.K. Gupta, R.N. Goyal, R.A. Sharma, Novel PVC membrane based alizarin sensor and its application: determination of vanadium, zirconium and molybdenum, Int. J. Electrochem. Sci. 4 (2009) 156–172.

[5] V.K. Gupta, A.K. Jain, L.P. Singh, U. Khurana, Porphyrins as carrier in PVC based membrane potentiometric sensors for nickel(II), Anal. Chim. Acta 355 (1997) 33–41.

[6] V.K. Gupta, M.A. Khayat, A.K. Singh, M.K. Pal, Nano level detection of Cd(II) using poly(vinyl chloride) based membranes of Schiff bases, Anal. Chim. Acta 634 (2009) 36–43.

[7] V.K. Gupta, S. Chandra, H. Lang, A highly selective mercury electrode based on a diamine donor ligand, Talanta 66 (2005) 575–580.

[8] V.K. Gupta, R. Jain, K. Radhapyari, N. Jadon, S. Agarwal, Voltammetric techniques for the assay of pharmaceuticals—a review, Anal. Biochem. 408 (2011) 179–196.

[9] V.K. Gupta, A.K. Jain, Pankaj Kumar, PVC-based membranes of N, N′-dibenzyl-1,4,10,13-tetraoxa-7,16-diazacyclooctadecane as Pb(II)-selective sensor, Sensors Actuators B Chem. 120 (2006) 259–265.

[10] R.N. Goyal, V.K. Gupta, S. Chatterjee, A sensitive voltammetric sensor for determination of synthetic corticosteroid triamcinolone, abused for doping, Biosens. Bioelectron. 24 (2009) 3562–3568.

[11] V.K. Gupta, S. Chandra, R. Mangla, Dicyclohexano-18-crown-6 as active material in PVC matrix membrane for the fabrication of cadmium selective potentiometric sensor, Electrochim. Acta 47 (2002) 1579–1586.

[12] V.K. Gupta, R. Prasad, A. Kumar, Preparation of ethambutol–copper(II) complex and fabrication of PVC based membrane potentiometric sensor for copper, Talanta 60 (2003) 149–160.

[13] V.K. Gupta, A.K. Jain, G. Maheshwari, H. Lang, Z. Ishtaiwi, Copper(II)-selective potentiometric sensors based on porphyrins in PVC matrix, Sensors Actuators B Chem. 117 (2006) 99–106.

[14] R.N. Goyal, V.K. Gupta, N. Bachheti, Fullerene-C60-modified electrode as a sensitive voltammetric sensor for detection of nandrolone—an anabolic steroid used in doping, Anal. Chim. Acta 597 (2007) 82–89.

[15] R.N. Goyal, V.K. Gupta, S. Chatterjee, Fullerene-C60-modified edge plane pyrolytic graphite electrode for the determination of dexamethasone in pharmaceutical formulations and human biological fluids, Biosens. Bioelectron. 24 (2009) 1649–1654.

[16] R.N. Goyal, V.K. Gupta, S. Chatterjee, Electrochemical oxidation of 2′,3′-dideoxyadenosine at pyrolytic graphite electrode, Electrochim. Acta 53 (2008) 5354–5360.

[17] V.K. Gupta, R. Prasad, P. Kumar, R. Mangla, New nickel(II) selective potentiometric sensor based on 5,7,12,14-tetramethyldibenzotetraazaannulene in a poly(vinyl chloride) matrix, Anal. Chim. Acta 420 (2000) 19–27.

[18] R. Jain, V.K. Gupta, N. Jadon, K. Radhapyari, Voltammetric determination of cefixime in pharmaceuticals and biological fluids, Anal. Biochem. 407 (2010) 79–88.

[19] V.K. Gupta, A.K. Jain, P. Kumar, S. Agarwal, G. Maheshwari, Chromium(III)-selective sensor based on tri-o-thymotide in PVC matrix, Sensors Actuators B Chem. 113 (2006) 182–186.

[20] R.N. Goyal, V.K. Gupta, S. Chatterjee, Simultaneous determination of adenosine and inosine using single-wall carbon nanotubes modified pyrolytic graphite electrode, Talanta 76 (2008) 662–668.

[21] V.K. Gupta, A.K. Singh, S. Mehtab, B. Gupta, A cobalt(II)-selective PVC membrane based on a Schiff base complex of N, N′-bis(salicylidene)-3,4-diaminotoluene, Anal. Chim. Acta 566 (2006) 5–10.

[22] V.K. Gupta, A.K. Singh, M.A. Khayat, B. Gupta, Neutral carriers based polymeric membrane electrodes for selective determination of mercury (II), Anal. Chim. Acta 590 (2007) 81–90.

[23] M. Fokkens, T. Schrader, F.G. Klarner, A molecular tweezer for lysine and arginine, J. Am. Chem. Soc. 127 (2005) 14415–14421.

[24] R.X. Peng, L.L. Lin, X.X. Wu, X.H. Liu, X.M. Feng, Fluorescent sensor based on BINOL for recognition of cysteine, homocysteine, and glutathione, J. Org. Chem. 78 (2013) 11602–11605.

[25] X. Chen, T. Pradhan, F. Wang, J.S. Kim, J. Yoon, Fluorescent chemosensors based on spiroring-opening of xanthenes and related derivatives, Chem. Rev. 112 (2012) 1910–1956.

[26] M.M. Song, Z.Y. Sun, C.P. Han, D.M. Tian, H.B. Li, L. Jiang, Design and fabrication of a biomimetic nanochannel for highly sensitive arginine response in serum samples, Chem. Eur. J. 20 (2014) 1–8.

[27] Y. Zhou, J. Yoon, Recent progress in fluorescent and colorimetric chemosensors for detection of amino acids, Chem. Soc. Rev. 41 (2012) 52–67.

[28] M. Sheliakina, V. Arkhypova, O. Soldatkin, O. Saiapina, B. Akata, S. Dzyadevych, Urease-based ISFET biosensor for arginine determination, Talanta 121 (2014) 18–23.

[29] R. Nishiyabu Jr., P. Anzenbacher, 1,3-Indane-based chromogenic calixpyrroles with push–pull chromophores: synthesis and anion sensing, Org. Lett. 8 (2006) 359–362.

[30] X.F. Shang, Y.L. Wang, X.F. Wei, Z.Y. Fu, J.L. Zhang, X.F. Xu, Synthesis and binding ability of molecular probes based on a phenanthroline derivative: theory and experiment, Molecules 18 (2013) 14840–14848.

[31] A.A. Beharry, G.A. Woolley, Azobenzene photoswitches for biomolecules, Chem. Soc. Rev. 40 (2011) 4422–4437.

[32] P. Li, Y.-M. Zhang, Q. Lin, J.-Q. Li, T.-B. Wei, A novel colorimetric HSO_4^- sensor in aqueous media, Spectrochim. Acta A Mol. Biomol. Spectrosc. 90 (2012) 152–157.

[33] X. Duan, T.M. Fu, J. Liu, C.M. Lieber, Nanoelectronics-biology frontier: from nanoscopic probes for action potential recording in live cells to three-dimensional cyborg tissues, Nano Today 8 (2013) 351–373.

[34] F. Taraballi, L. Russo, C. Battocchio, G. Polzonetti, F. Nicotra, L. Cipolla, A model study for tethering of (bio)active molecules to biomaterial surfaces through arginine, Org. Biomol. Chem. 12 (2014) 4089–4992.

[35] B. Romana, M. Batger, C.A. Prestidge, G. Colombo, F. Sonvico, Expanding the therapeutic potential of statins by means of nanotechnology enabled drug delivery systems, Curr. Top. Med. Chem. 14 (2014) 1182–1193.

[36] C. Bonini, L. Chiummiento, M. Funicello, M.T. Loparda, P. Lupattelli, A. Lautita, A. Cornia, Novel chiral calix[4]arenes by direct asymmetric epoxidation reaction, J. Org. Chem. 73 (2008) 4233–4236.

[37] J. Shao, H. Lin, H.K. Lin, A novel chromo- and fluorogenic dual responding $H_2PO_4^-$ receptor based on an azo derivative, Dyes Pigments 80 (2009) 259–263.

[38] X. Zhang, K. Zou, C.S. Lee, S.T. Lee, Single-crystal nanoribbons, nanotubes, and nanowires from intramolecular charge-transfer organic molecules, J. Am. Chem. Soc. 129 (2007) 3527–3533.

[39] A.J. Gesquiere, T. Uwada, T. Asahi, H. Masuhara, P.F. Barbara, Single molecule spectroscopy of organic dye nanoparticles, Nano Lett. 5 (2005) 1321–1325.

[40] X.J. Peng, Y.K. Wu, J.L. Fan, M.Z. Tian, K.L. Han, Colorimetric and ratiometric fluorescence sensing of fluoride: tuning selectivity in proton transfer, J. Org. Chem. 70 (2005) 10524–10531.

[41] Z.H. Lin, Y.G. Zhao, C.Y. Duan, B.G. Zhang, Z.P. Bai, A highly selective chromo- and fluorogenic dual responding fluoride sensor: naked-eye detection of F^- ion in natural water via a test paper, Dalton Trans. 30 (2006) 3678–3684.

[42] Z. Xu, S. Kim, K.H. Lee, J. Yoon, A highly selective fluorescent chemosensor for dihydrogen phosphate via unique excimer formation and PET mechanism, Tetrahedron Lett. 48 (2007) 3797–3800.

[43] G.S. Kumar, D.C. Neckers, Photochemistry of azobenzene-containing polymers, Chem. Rev. 89 (1989) 1915–1925.

[44] J. Harada, T. Fujiwara, K. Ogawa, Crucial role of fluorescence in the solid-state thermochromism of salicylideneanilines, J. Am. Chem. Soc. 129 (2007) 16216–16221.

[45] Y. Liu, B.H. Han, H.Y. Zhang, Spectroscopic studies on molecular recognition of modified cyclodextrins, Curr. Org. Chem. 8 (2004) 35–46.

[46] Y. Liu, C.C. You, H.Y. Zhang, Supramolecular Chemistry, Nankai University Publication, Tianjin, 2001.

[47] J. Bourson, J. Pouget, B. Valeur, Ion-responsive fluorescent compounds. 4. Effect of cation binding on the photophysical properties of a coumarin linked to monoaza- and diaza-crown ethers, J. Phys. Chem. 97 (1993) 4552–4557.

[48] M.J. Frisch, G.W. Trucks, H.B. Schlegel, G.E. Scuseria, M.A. Robb, J.R. Cheeseman, J.A. Montgomery Jr., T. Vreven, K.N. Kudin, J.C. Burant, J.M. Millam, S.S. Iyengar, J. Tomasi, V. Barone, B. Mennucci, M. Cossi, G. Scalmani, N. Rega, G.A. Petersson, H. Nakatsuji, M. Hada, M. Ehara, K. Toyota, R. Fukuda, J. Hasegawa, M. Ishida, T. Nakajima, Y. Honda, O. Kitao, H. Nakai, M. Klene, X. Li, J.E. Knox, H.P. Hratchian, J.B. Cross, C. Adamo, J. Jaramillo, R. Gomperts, R.E. Stratmann, O. Yazyev, A.J. Austin, R. Cammi, C. Pomelli, J.W. Ochterski, P.Y. Ayala, K. Morokuma, G.A. Voth, P. Salvador, J.J. Dannenberg, V.G. Zakrzewski, S. Dapprich, A.D. Daniels, M.C. Strain, O. Farkas, D.K. Malick, A.D. Rabuck, K. Raghavachari, J.B. Foresman, J.V. Ortiz, Q. Cui, A.G. Baboul, S. Clifford, J. Cioslowski, B.B. Stefanov, G. Liu, A. Liashenko, P. Piskorz, I. Komaromi, R.L. Martin, D.J. Fox, T. Keith, M.A. Al-Laham, C.Y. Peng, A. Nanayakkara, M. Challacombe, P.M.W. Gill, B. Johnson, W. Chen, M.W. Wong, C. Gonzalez, J.A. Pople, Gaussian, Inc., Pittsburgh PA. 2003.

[49] P. Gonil, W. Sajomsang, U.R. Ruktanonchai, P.N. Ubol, A. Treetong, P. Opanasopit, S. Puttipipatkhachorn, Synthesis and fluorescence properties of N-substituted 1-cyanobenz[*f*]isoindole chitosan polymers and nanoparticles for live cell imaging, Biomacromolecules 15 (2014) 2879–2888.